Roughening-induced deconstruction in (100) facets of CsCl-type crystals

Douglas Davidson and Marcel den Nijs
Department of Physics, University of Washington, Seattle, Washington 98195
(Received 13 August 1996)

The staggered six-vertex model describes the competition between surface roughening and reconstruction in (100) facets of CsCl-type crystals. Its phase diagram does not have the expected generic structure, due to the presence of a fully packed loop-gas line. We prove that the reconstruction and roughening transitions, cannot cross nor merge with this loop-gas line if these degrees of freedom interact weakly. However, our numerical finite size scaling analysis shows that the two critical lines merge along the loop-gas line, with strong-coupling scaling properties. The central charge is much larger than 1.5 and roughening takes place at a surface roughness much larger than the conventional universal value. It seems that additional fluctuations become critical simultaneously. [S1063-651X(97)13001-X]

PACS number(s): 64.60.Fr, 68.35.Rh, 82.65.Dp, 68.35.Bs

I. INTRODUCTION

In a recent paper, Mazzeo, Carlon, and van Beijeren [1] discussed the competition between surface roughening and reconstruction in $c(2\times2)$-reconstructed (100) facets of CsCl-type crystals. Their numerical finite size scaling (FSS) results for the staggered six-vertex model are quite surprising. The phase diagram lacks a so-called reconstructed rough (RR) phase, although such a phase is a generic feature in surfaces where step excitations do not destroy the reconstruction order. The phase diagram should have the same structure as for missing row (MR)-reconstructed simple-cubic (sc) (100) facets [2–4]. The roughening and reconstruction lines should be able to cross. Instead they only seem to approach each other exponentially closely. In this paper, we explain why this happens. The absence of a RR phase in the staggered six-vertex model is accidental, the result of a special symmetry of the interactions in this particular model, the presence of a fully packed loop-gas line.

In Sec. II, we review the rich history of the staggered six-vertex model. In Sec. III, we describe the topological properties of step and wall excitations in $c(2\times2)$-reconstructed CsCl(100). We set up the cell-spin model description for this type of competition between surface roughening and reconstruction. Topological considerations determine whether the roughening and reconstruction lines can cross or only merge (whether an RR phase is possible or not). For example, in MR-reconstructed sc(110) facets they can cross, but in MR-reconstructed fcc(110) facets they can only merge [2–4]. We show that in $c(2\times2)$ reconstructed CsCl(100) they are allowed to cross. The competition in this surface is in the same universality class as in MR-reconstructed sc(110) facets. However, the RR phase in the staggered six-vertex model is at best narrow. We estimate the energies of two topologically distinct types of steps, and find that they cost almost the same energy in the region of the phase diagram where the surface roughens.

Carlon and co-workers [5,6] pointed out the existence of a special line in the phase diagram. It runs in between the Ising and roughening lines. Along this line the partition function is equivalent to the four-state Potts model on a square lattice with negative Boltzmann weights. They expected this line to be similar to a so-called disorder line, and this explains their numerical results (the noncrossing of the Ising and roughening lines). In Sec. IV we show that this line is equivalent to a fully packed loop gas on a square lattice.

In Sec. V, we prove rigorously that the reconstruction line cannot cross the loop-gas line. Furthermore, we show that the roughening line also cannot cross the loop-gas line if the roughening and reconstruction degrees of freedom couple weakly. The weak-coupling hypothesis assumes that the reconstruction and roughening degrees of freedom interact weakly, such that their scaling properties are a superposition. Earlier studies of models for MR-reconstructed sc(110) and fcc(110) facets strongly support the weak-coupling hypothesis [2–4]. It should hold for CsCl(100) as well, since the cell-spin model in Sec. III is the same.

This seems to resolve the issue. The phase diagram found by Mazzeo, Carlon, and van Beijeren [1] is the only one allowed within weak-coupling theory, but it is an accident. The special symmetries of the loop-gas line cause this particular model to follow a special cut through the generic phase diagram. The roughening and Ising lines approach each other only pathologically closely, because entropy cannot be lowered far enough to reach the crossing point into the RR phase. In general, the interactions in CsCl-type surfaces will be more generic, and allow the RR phase. However, this is not the end of the story.

In Sec. VI we present our numerical FSS results. Mazzeo, Carlon, and van Beijeren [1] performed their study before they discovered the loop-gas line. Knowledge of the exact location of the line where the roughening and reconstruction lines must merge or cross (if they do so) enhances the accuracy of the analysis considerably. We find that the scaling behavior along the loop-gas line does not obey the weak-coupling hypothesis.

The question of weak versus strong-coupling-type competition between reconstruction and roughening degrees of freedom is an important unresolved issue in the theory of two-dimensional (2D) critical phenomena. It appears not only in surface physics, but also, e.g., in coupled Josephson junction arrays in a magnetic field (the fully frustrated XY model) [7–13]. The phase diagrams of these problems share as a basic feature a conventional order-disorder transition

line (such as an Ising or three-state Potts transition), approaching a critical (rough) phase. A critical line described by conformal field theory (CFT) with central charge $c<1$ competes with a critical phase with central charge $c=1$. The fundamental question is whether interesting CFT's can result from this competition. The c theorem [14,15] implies that such CFT's must have a central charge lower than 1. The ones we know are rather simple direct products of $c=1$ and $c<1$ theories, some with extra symmetries, such as supersymmetry, between the two types of degrees of freedom. This supports the weak-coupling hypothesis. However, do more interesting types of $c>1$ CFT's really not exist? Can the coupling between two types of $c\leqslant 1$ degrees of freedom ever lead to more intricate $c>1$ scaling behavior? This question is the driving force behind a large number of numerical studies, in particular within the context of the fully frustrated XY model and the competition between surface roughening and reconstruction [1–13]. But this has proved to be extremely difficult to answer.

Three types of answers are possible and each has appeared in the literature. The first one is that the $c<1$ line cannot reach the $c=1$ phase. The line can only approach this phase pathologically close. This suggests the existence of a no-go theorem of some sort. Our exact results in Sec. V amount to such a no-go theorem, but only for the staggered six-vertex model, and only within the weak-coupling hypothesis.

The second possibility is the weak-coupling scenario. The reconstruction and roughening lines cross or merge, but the two types of critical fluctuations interact weakly and behave like a direct product. The central charge is equal to the sum ($c=1.5$ in our case, since $c=0.5$ at Ising critical points, and $c=1$ inside the rough phase). This type of behavior is almost indistinguishable from the effective scaling when the two lines approach each other only pathologically close (see Sec. V). Typically, the numerical data can be interpreted both ways [7–13]. Fortunately, our exact results in Sec. V distinguish between the two in the six-vertex model.

The third possibility is that the lines cross or merge with a scaling behavior different from a simple superposition. The central charge is not equal to the sum. Convincing evidence for strong coupling would revolutionize CFT at $c>1$. Numerical evidence of strong coupling has been presented in models related to the fully frustrated XY model, but remains ambiguous [7–13]. We find strong numerical evidence (in Sec. VI) that the roughening and reconstruction lines in the staggered six-vertex model merge along the loop-gas line, with strong-coupling scaling properties.

In Sec. VII, we summarize our results, discuss related recent results for fully packed loop gases on different lattices, and give a possible explanation for the strong-coupling behavior.

II. STAGGERED SIX-VERTEX MODEL

The (100) facets of CsCl-type crystals have a body-centered-type stacking with two kinds of atoms, types A and B. The appropriate solid-on-solid description is a staggered body-centered solid-on-solid (BCSOS) model, equivalent to a staggered six-vertex model. Stacks of A occupy the A sublattice, where the column heights are odd numbers,

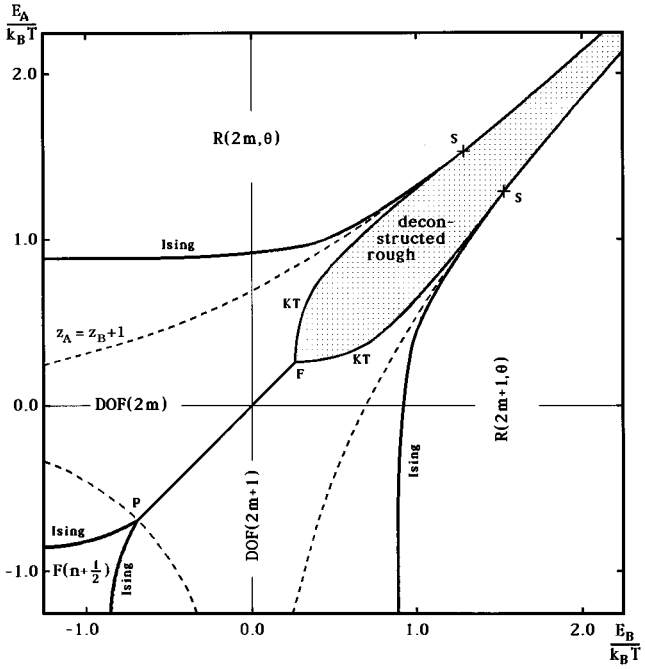

FIG. 1. Phase diagram of the staggered six-vertex model defined in Eq. (1). At point S the Ising reconstruction and KT roughening lines merge into a single transition along the loop-gas line (dashed).

$h_A=\pm 1, \pm 3, \pm 5, \ldots$. The B-type atoms occupy the B sublattice where the column heights are even, $h_B=0, \pm 2, \pm 4, \ldots$. Nearest-neighbor stacks differ in height by only one unit, $dh=\pm 1$. The surface energy is given by

$$\mathcal{H}=-\frac{1}{4}\sum_{x,y}\{E_A(h_{(x,y)}-h_{(x+1,y\pm 1)})^2 + E_B(h_{(x+1,y)}-h_{(x,y\pm 1)})^2\}. \quad (1)$$

The summation runs over only the A-type sublattice sites (all even values of $x+y$).

This model has a rich history. Figure 1 shows its phase diagram. It is exactly soluble by the Bethe ansatz along the line $E_A=E_B$, where it reduces to the so-called F model [16–18]. We denote the flat phase as $F(n+\frac{1}{2})$, because the average surface height is a half-integer. A more detailed notation is in terms of the heights at four sublattices $(h_{A,+},h_{A,-};h_{B,+},h_{B,-})=(n+1,n+1;n,n)$. The $+$ and $-$ indices represent the two (checkerboard type) sublattices within each A and B sublattice. Along $E_A=E_B$, elementary step excitations induce a height change ± 1. They roughen the surface at $z_A=z_B=\frac{1}{2}$, with $z_A=\exp(E_A/k_BT)$ and $z_B=\exp(E_B/k_BT)$ [16–18].

E_A and E_B are not equal in CsCl-type surfaces, since the A- and B-type atoms interact differently. Knops [19] realized that this changes the disordering of the $F(n+\frac{1}{2})$ phase. He used the equivalence of Eq. (1) to the Ashkin-Teller model. Rephrased from the more recent perspective of preroughening (PR) transitions and disordered flat (DOF) phases, his results are as follows: $F(n+\frac{1}{2})$ contains two types of steps, S_A and S_B. In surfaces with a height $2m+\frac{1}{2}$, up-steps are of type S_B and down-steps are of type S_A (they reverse roles in surfaces with a height $2m-\frac{1}{2}$). $-E_A$ is the energy of S_A

steps (per unit length), and $-E_B$ of S_B steps. The free energy of S_A steps vanishes before that of S_B steps on the $E_A > E_B$ side of the phase diagram. This does not cause roughening yet, since building up a slope in the surface requires S_B steps as well. Only the spontaneous symmetry breaking between pairs of surface heights, $2m+\frac{1}{2}$ and $2m-\frac{1}{2}$, is lifted. The result is a DOF phase with lots of S_A-type steps in the surface, but still flat at large length scales. In Fig. 1, we denote this as the DOF $(2m)$ phase, because the average surface height is an even integer, $2m$.

This is an example of PR transition, but in a different universality class than the conventional one [2,4]. In both cases the average surface height changes spontaneously by half a unit. At conventional PR transitions the number of degenerate equivalent surface heights does not change. They all shift by one-half unit, and the distance between them remains the same. In this example, however, the distance between degenerate equivalent surface heights increases from 1 to 2. The elementary step height is equal to $dh=\pm 1$ in the $F(n+\frac{1}{2})$ phase, but equal to $dh=\pm 2$ in the DOF $(2m)$ phase. Therefore, this is a simple Ising line instead of a line with continuously varying critical exponents.

This doubling in the basic step height not only changes the nature of the transition into the DOF phase; it also delays the roughening transition considerably, even for small energy differences E_A-E_B [19]. The surface roughness is characterized by the amplitude of the height-height correlations as

$$\langle (h_{\mathbf{r}+\mathbf{r}_0}-h_{\mathbf{r}_0})^2\rangle \simeq \frac{1}{\pi K_G}\ln(|\mathbf{r}|), \tag{2}$$

where K_G^{-1} is the surface roughness parameter. Rough phases become unstable with respect to discreteness of the surface height at $K_G=\pi/8$ for a step size $dh=\pm 2$ compared to $K_G=\pi/2$ for a step size $dh=\pm 1$, in other words, not until the surface is four times as rough. In this particular model, these roughening lines lie at the side of the phase diagram where both step energies are negative (both E_A and E_B are positive). Point F in Fig. 1 is located at $z_A=z_B=\sqrt{(1+\frac{1}{2}\sqrt{2})}=1.306\,56$. The local structure of the phase diagram around point F is known as a ''critical fan'' [20]. Notice that unreconstructed surfaces described by Eq. (1) never roughen (except along $E_A=E_B$). They follow specific paths through Fig. 1, which are approximately lines at constant E_A/E_B with both E_A and E_B negative. Such lines do not enter the critical fan. The absence of a roughening transition is not a generic feature, however. Experimental unreconstructed CsCl(100)-type surfaces will include step-step interactions and other aspects that are able to move point F toward $z_A=z_B=1$ and beyond.

In the upper left corner of Fig. 1 the surface reconstructs. All B-type columns are at the same height, $2m$, and the A-type columns alternate between $2m\pm 1$; e.g., $(h_{A+}, h_{A-}, h_{B+}, h_{B-})=(2m+1, 2m-1, 2m, 2m)$. We call this the $R_A(2m,\theta)$-reconstructed phase. The average surface height is an even integer. The Ising-type order parameter $\theta=0,\pi$ denotes which of the two A-type sublattices is on top. The average surface height is the same as in the DOF $(2m)$ phase. The difference is the appearance of antiferromagnetic-type ordering of the A-sublattice heights. The competition between deconstruction of this type of order and surface roughening is the topic of this paper, in particular the existence of point S in Fig. 1, and the scaling properties of the critical line beyond this point.

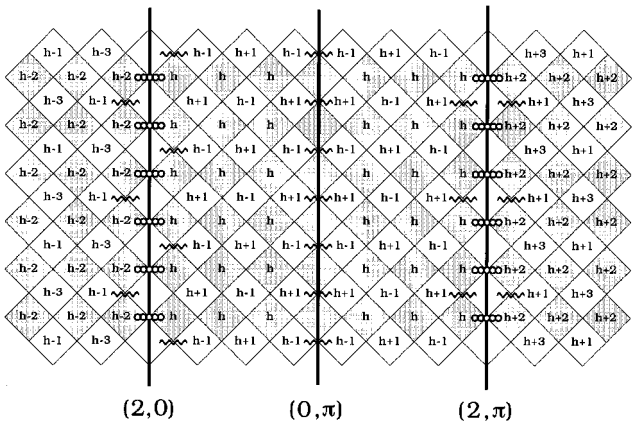

FIG. 2. Excitations inside the $R_A(2m,\theta)$-reconstructed phase: a (2,0) step, $(0,\pi)$ wall, and $(2,\pi)$ step running in the diagonal direction. The shaded areas represent the B sublattice. The wiggly (circled) lines represents E_A- (E_B)-type broken bonds.

Figure 1 has mirror symmetry with respect to $E_A=E_B$. The A- and B-type particles switch roles. In the lower right corner of Fig. 1 the surface height is an odd integer. The surface reconstructs into an $R_B(2m+1,\theta)$ phase, and the DOF phase is of type DOF $(2m+1)$.

III. STEPS AND WALLS IN THE $c(2\times 2)$ PHASE

Reconstructed surfaces can disorder in several ways: they can lose their reconstruction first and then roughen; they can roughen first and only later deconstruct; or roughening can induce a simultaneous deconstruction transition. The latter happens when the topology of the surface implies that steps destroy the reconstruction order parameter. Figure 2 shows the three topologically distinct line excitations in the $R_A(2m,\theta)$ phase: a $(+2,\pi)$ step, a $(0,\pi)$ wall, and a $(-2,0)$ step. Wall excitations do not change the surface height. They cause a switch in which of the two A-type sublattices is on top. Steps of type $(\pm 2,0)$ change the surface height by ± 2, but do not change the Ising order parameter θ; the same A-type sublattice stays on top. Steps of type $(\pm 2,\pi)$ change the surface height by ± 2, and switch which of the two A-type sublattices is on top.

It is an illusion to think that $(\pm 2,\pi)$ steps destroy the reconstruction order. They preserve a different definition of the reconstruction order. This can be expressed in terms of which sublattice is on top, $\theta=0,\pi$, or in terms of parity spins, $S_A=\exp[\frac{1}{2}i\pi h_A]=\pm 1$. The S_A spins are ordered antiferromagnetically in the $R_A(2m,\theta)$ phase. These two definitions of the Ising order are equivalent to flat surfaces but inequivalent in rough surfaces. The $(\pm 2,\pi)$ steps destroy the sublattice order but preserve the parity order. The $(\pm 2,0)$ steps destroy the parity order but preserve the sublattice order. Two types of RR phases are possible: the surface is rough, but such that the S_A order parameter remains nonzero; or the surface is rough, but such that the θ order parameter persists. In diffraction experiments, the roughening transition can be

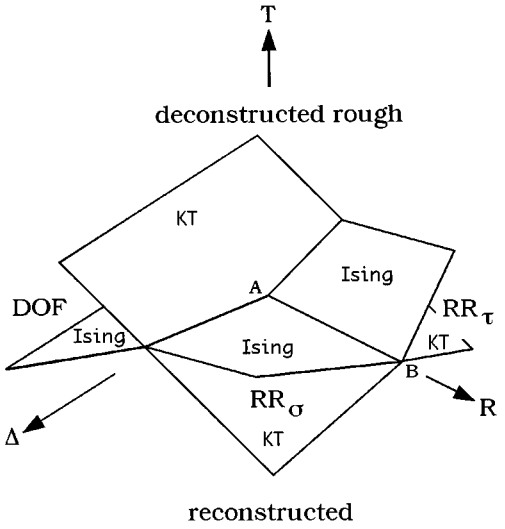

FIG. 3. Generic phase diagram for the competition between surface roughening and the Ising-type reconstruction [see Eq. (3)], with Δ the energy difference between (2,0)- and $(2,\pi)$-type steps, and R the difference between the energy of a $(0,\pi)$ wall and the average step energy.

easily mistaken for a simultaneous deconstruction transition. The ''reconstruction diffraction peak'' couples only to one of the two order parameters (typically the parity one), and that order might not be the type that persists in the RR phase.

Along paths where either type of step costs less energy than a wall, the surface roughens first, into the appropriate RR phase, followed by an Ising-type deconstruction transition inside the rough phase. Along paths where walls cost less than steps, the surface deconstructs into the DOF $(2m)$ phase, and only later roughens.

Figure 3 illustrates these different typical behaviors. It is a schematic phase diagram for the following model [4]. Each site of a square lattice contains an Ising spin, $\sigma_{\mathbf{r}}=\pm 1$, and a height variable, $h_{\mathbf{r}}=0,\pm 2,\pm 4,\ldots$. They interact as

$$\mathcal{H}=-\sum_{\langle \mathbf{r},\mathbf{r}'\rangle} K_\sigma \sigma_{\mathbf{r}}\sigma_{\mathbf{r}'}+\frac{1}{2}(K_\tau \sigma_{\mathbf{r}}\sigma_{\mathbf{r}'}+K_h)[2-(h_{\mathbf{r}}-h_{\mathbf{r}'})^2], \tag{3}$$

with $\mathbf{r}$ and $\mathbf{r}'$ nearest-neighbor sites. Only steps of height $dh=\pm 2$ are allowed. $\sigma_{\mathbf{r}}=\cos(\pi\theta_r)=\pm 1$ represents the sublattice-type reconstruction order parameter, and $h_{\mathbf{r}}$ the local surface height. Walls cost $E(0,\pi)=2(K_\sigma+K_\tau)$. Steps cost $E(2,0)=2(K_\tau+K_h)$ and $E(2,\pi)=2(K_\sigma+K_h)$, respectively. This is a renormalized effective model, on a larger length scale than the staggered six-vertex model. It must be in the same universality class in the local neighborhood about the reconstructed phase, assuming we correctly identify all critical fluctuations of the six-vertex model in this part of the phase diagram. Figure 1 should follow a specific 2D cut through Fig. 3.

The mirror symmetry in Fig. 3 with respect to $\Delta=E(2,0)-E(2,\pi)$ reflects the equivalence between the two definitions of the reconstruction order. Consider the following construction of a typical configuration. Define a second type of Ising spin $S_{\mathbf{r}}=\exp(\frac{1}{2}i\pi h_{\mathbf{r}})=\pm 1$, and draw σ- and S-type Bloch walls along the bonds of the lattice. The σ-type Bloch walls represent wall excitations in the surface, and the S-type Bloch walls represent (2,0)-type steps. Place one arrow along each S-type Bloch wall to denote the direction in which the height changes across the steps (up from left to right while looking in the direction along the arrow). Sections along the lattice where S- and σ-type Bloch walls coincide represent $(2,\pi)$-type steps. The following change of variables generates the mirror symmetry in Fig. 3. Define Ising spins $\tau=\sigma S$ to represent the $(2,\pi)$-type steps and then eliminate the σ spins, $(\sigma,S)\rightarrow(\tau,S)$. This leads us back to Eq. (3), but with the τ spins replacing the σ spins, and with $K_\alpha\leftrightarrow K_\tau$. The two RR phases switch places.

This transformation is reminiscent of supersymmetry between the fermion (Ising) and boson (height) degrees of freedom. It is weaker than supersymmetry, only a Z_2-type invariance [4]. At the same time it is more general, an exact symmetry of the lattice model not restricted to T_c. The entire $\Delta=0$ space is invariant, instead of only the critical line $A-B$. We expect that critical fluctuations generate full supersymmetry at large length scales. The roughening-induced simultaneous deconstruction transition along A-B will then be described by a supersymmetric CFT, probably one with central charge $c=1.5$ where the roughening and reconstruction are weakly coupled.

Experimental systems and microscopic models follow specific cuts through Fig. 3. For example, the antiferromagnetic restricted solid-on-solid model describes checkerboard-type-reconstructed sc(100) facets [2,4]. Indeed, its phase diagram represents a generic slice out of Fig. 3 with a DOF phase and an RR phase; and the Ising and roughening degrees couple weakly with central charge $c=1.5$ [2,4]. One of the exactly soluble generalized RSOS models [21] moves along the Ising surface in Fig. 3 as well, and confirms weak-coupling behavior [22]. A third example is the chiral four-state clock-step model [4] which describes MR-reconstructed fcc(110) facets. Topology requires the two types of steps in those surfaces to have identical energies. The nonchiral limit of the four-state clock-step model coincides with the $\Delta=0$ plane of Eq. (3). Numerical evidence supports the expectation that along A-B the Ising and roughening degrees of freedom couple weakly with $c=1.5$.

The phase diagram of the staggered six-vertex model should be a generic cut through Fig. 3, similar to the RSOS model. There is no intrinsic topological requirement for Δ to be zero. However, Mazzeo, Carlon, and van Beijeren did not find an RR phase.

One possible explanation is that Δ is small or vanishes ''accidentally'' in the six-vertex model. The wall and steps in Fig. 2 run diagonally across the surface. In that direction, the two types of steps cost the same amount of energy per unit length, $E(2,0)=E(2,\pi)=\frac{1}{2}\sqrt{2}(2E_A-E_B)$. A wall cost $E(0,\pi)=\frac{1}{2}\sqrt{2}E_A$. This suggests that Δ is equal to zero. However, Δ is quite large for walls and steps running in the horizontal and vertical direction: $(0,\pi)$ walls cost $E(0,\pi)=E_A$ per unit length, (2,0) step cost $E(2,0)=E_A-E_B$, and $(2,\pi)$ steps exist only as composite objects [a (2,0) step followed by a $(0,\pi)$ wall, i.e., $E(2,\pi)=2E_A-E_B$].

Walls tend to run in the diagonal direction, but steps switch direction. Deep inside the $R(2m,\theta)$ phase to the left of the line $E_A/E_B\simeq -0.7$ the steps tend to run in the diagonal

direction. Δ is small, but this is the part of the phase diagram where the walls cost much less energy. The surface deconstructs into the DOF $(2m)$ phase before it roughens. Along $z_B=0$ the model reduces to the Ising model, and therefore the deconstruction transition takes place at $z_A=1+\sqrt{2}$. In the zeroth order approximation, the deconstruction line is located at $z_A=1+\sqrt{2}$ for all E_B, since the wall energy does not involve E_B.

Deep inside the $R(2m,\theta)$ phase to the right of the line $E_A/E_B\simeq-0.7$, steps tend toward vertical and horizontal directions. The (2,0) steps are most favorable, and Δ is large. However, roughening cannot take place until E_B and E_A are of the same order of magnitude. Roughening takes place at approximately $\exp[E(2,0)/k_BT_R]\simeq1+\sqrt{2}$ (the Ising formula gives reasonable estimates for transition temperatures in general). We can construct two different estimates for the roughening line in Fig. 1, by assuming (2,0) steps run vertically or diagonally. These estimates are quite close to each other. This means that near the roughening transition the $E(2,0)$ steps run almost equally likely in the diagonal direction as in the horizontal or vertical directions. Δ must be small near the roughening transition. $E(2,\pi)$ steps come into play, and the RR phase is narrow at best.

IV. FULLY PACKED LOOP GAS ON A SQUARE LATTICE

Carlon and co-workers [5,6] realized recently that along the lines $z_A+z_B=1$ and $z_A=z_B\pm1$ (the dashed lines in Fig. 1) the staggered six-vertex model maps onto the four-state Potts model, and that the $z_A=z_B+1$ line seems to lie in between the Ising and Kosterlitz-Thouless (KT) roughening lines. This mapping has been known actually for a long time but not from this perspective. For details, we refer to the original source [23]. Carlon and van Beijeren [6] expect that the Potts line will turn out to be a type of disorder line, and thus will explain that the Ising and roughening lines cannot meet, in accordance with their numerical results [1]. The properties of this line are much more intriguing. The essential observation is that along the Potts line the six-vertex model reduces to a fully-packed (FP) loop-gas.

In the six-vertex representation of the BCSOS model, an arrow points along each bond of the lattice, to denote the height difference between nearest-neighbor columns $h_A-h_B=\pm1$. Figure 4(a) shows the six allowed vertex states. In the loop-gas model every bond contains a loop segment. The loops follow the bonds of the lattice, are closed, and do not intersect. It is a fully packed loop gas. Figure 4(b) shows the two possible vertex states, A and B. The partition function is of the form

$$Z=\sum_{\mathcal{G}} z_A^{N_A}z_B^{N_B}2^{N_L}=z_A^{N_V}\sum_{\mathcal{G}} x^{N_B}2^{N_L}, \tag{4}$$

with the summation over all FP loop-graphs $\mathcal{G}$, $x=z_B/z_A$, N_A the number of vertices of type A, N_B the number of vertices of type B, $N_V=N_A+N_B$ the total number of vertices in the lattice, and N_L the number of loops. The fugacity factors of 2 can be counted by placing arrows on the loops; clockwise and anticlockwise arrows. Loop configurations with such arrows resemble configurations in the six-vertex model, but

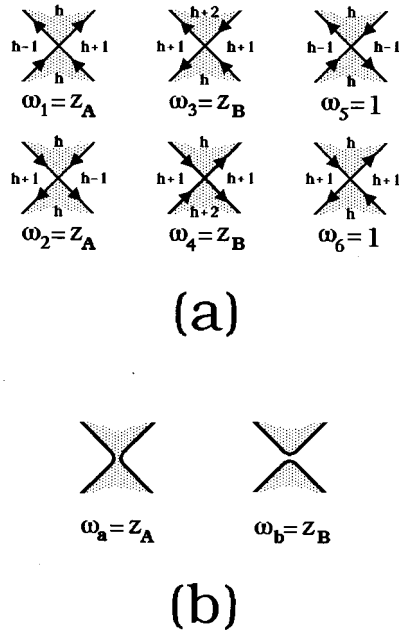

FIG. 4. The six vertex states of the six-vertex model (a), and the two vertex states of the loop-gas model (b), with their Boltzmann weights.

they are not one-to-one related. Vertex states with antiparallel arrows, labeled 5 and 6 in Fig. 4(a), can be interpreted as both A- or B-type loop states. How to deal with this is one of the essential steps of the mapping of the Potts model onto the six-vertex model: each six-vertex configuration represents the sum over all possible loop-gas interpretations [23]. Still, the models are only identical along special lines. In the six-vertex model, vertex states 5 and 6 are assigned a Boltzmann factor $\omega_5=\omega_6=1$ (both next-nearest-neighbor heights are equal), while in the loop gas their weights are the sum over all loop interpretations: $\omega_5=\omega_6=z_A+z_B$. The staggered six-vertex model reduces to the FP loop gas, Eq. (4), only when these are equal, only along the line $z_A+z_B=1$.

All lines of type $\pm z_A+\pm z_B=1$ are FP loop gases as well, due to the fact that vertex states 1 and 2 (and also 3 and 4) in Fig. 4(a) always appear in pairs (Fig. 1 has mirror symmetry with respect to z_A and also z_B). The lines $z_A=z_B+1$ and $z_B=z_A+1$ represents loop gases with negative Boltzmann weights,

$$Z=\sum_{\mathcal{G}} (-1)^{N_B}z_A^{N_A}z_B^{N_B}2^{N_L}=z_A^{N_V}\sum_{\mathcal{G}} (-1)^{N_B}x^{N_B}2^{N_L}. \tag{5}$$

These two lines are analytic continuations of each other with $0\leqslant x<1$ along $z_A=z_B+1$, and $1\leqslant x<\infty$ along $z_B=z_A+1$; the minus signs in Eq. (5) can be counted equally well by N_B as N_A, since $N_A+N_B=N_V$ is a constant. FP loop gases have been a focus of attention recently [24–26]. In particular, the FP loop gas on a honeycomb lattice resembles Eq. (4). We will discuss possible connections with this recent work in Sec. VII.

In the loop gas, the arrows are merely a gimmick to count the loop fugacity. They are placed at random on each loop. Therefore it seems reasonable that any order associated with the up-down nature of the steps must be absent along the

loop-gas line, the reconstruction order as well as the surface flatness. This is too naïve. The surface is able to maintain flatness. Only the reconstruction order is absent. Notice that the loop-gas lines in Fig. 1 move through the DOF phases. The following visualization is quite useful. Interpret the B sublattices as ''patches of red-land'' and the A sublattice as ''patches of blue-land.'' The loops are the coastlines. The two vertex states in Fig. 4(b) represent the presence of either a bridge connecting the two patches of blue-land or the two patches of red-land. The fugacity factor 2 for each loop can be interpreted as a random height difference of $dh=\pm 1$ between blue- and red-lands at each coastline, while looking in the direction along the arrow the land on the left is lower by one unit than the land on the right. (The arrows attribute a helicity to each coast line.) At $z_A=0$ there exist only red-land bridges. All red patches are connected, and they are all at the same height; the surface stays flat. All blue patches are disconnected and randomly distributed at heights $h\pm 1$. Consequently, the reconstruction order is absent. Everywhere along the loop gas line inside the DOF $(2m)$ phase, there exists a large continent of red-land spanning the entire lattice, and keeping the surface flat. Moreover, all blue-lands are finite in size (lakes inside the red-land continent). The red- and blue-lands switch roles inside the DOF $(2m+1)$ phase. The only other possibility is that all red- and blue-land masses are finite in size. There the surface is rough and unreconstructed. The reconstruction order is always absent along the loop-gas line. In Sec. V we prove this rigorously.

V. INTERFACE FREE ENERGIES

Consider the six-vertex model partition function in a semi-infinite strip geometry, and the following boundary conditions (BC's): $h(x+N,y)=\pm h(x,y)+a$, with a an even integer. The lattice forms a cylinder, infinitely long in the y-direction and N lattice sites in circumference in the x direction. The free energy per unit strip width for each of these BC's, $f(\pm,a)$, can be calculated as the largest eigenvalue of the transfer matrix. The free energy differences $\eta(\pm,a)=f(\pm,a)-f(+,0)$ are related to specific step, wall, and other defect free energies.

For example, the $h(x+N,y)=h(x,y)+2$ BC forces a step into the $R_A(2m)$ reconstruction. To see this, visualize the $R_A(2m)$ ground state as a crisscross structure of horizontal and vertical intersecting straight lines. Each carries an arrow, pointing alternately up and down (to the left and right). Reversing all arrows interchanges the two degenerate $R_A(2m)$ states. Reversing the arrows along only one vertical line creates a step. This is a (2,0)-type step, not a $(2,\pi)$-type step, because the arrow reversal along this specific line does not affect the θ-type order parameter on either side of the step. The same A-type sublattice stays on top on either side. By reversing the arrow we create a net height difference across the surface of $a=\pm 2$. The $h(x+N,y)=h(x,y)+2$ BC matches this structure for even values of N, and therefore forces a (2,0) step into the surface along the entire cylinder. $\eta(+,2)$ is equal to the (2,0)-type step free energy everywhere inside the $R_A(2m)$ phase.

One method to force a wall excitation into the reconstructed phase is to apply periodic boundary conditions (PBC's), $h(x+N,y)=h(x,y)$, at odd strip widths N. To see this, visualize the $R_A(2m)$ ground state as an array of elementary loops with alternate helicity. In the red- and blue-land interpretation of the loop gas the $R_A(2m)$ ground state is the structure, in which all blue-lands are disconnected elementary lakes, and the height changes at the coast lines follow a strict up-down pattern. The coast line arrows have alternative helicity. We run the transfer matrix in the diagonal direction, where the reconstructed phase fits only onto the lattice if the strip width N is a multiple of 2. The $h(x+N,y)=h(x,y)$ BC frustrates the helicity order at odd strip widths. Therefore $\eta(+,0)_o$ is equal to the wall free energy.

The BC $h(x+N,y)=h(x,y)+2$ forces a $(2,\pi)$-type step into the reconstructed phase at odd strip widths. Other types of BC's have similar effects: twist boundary conditions (TBC's) at even values of N create a $(0,\pi)$ wall for $h(x+N,y)=-h(x,y)$, and a $(2,\pi)$-type step for $h(x+N,y)=-h(x,y)+2$.

Loop-gas lines in solid-on-solid models signal special properties. Free energies with certain boundary conditions become ''accidentally'' equal, implying that specific excitations have identical free energies. For example, the RSOS model contains a (non-fully-packed) loop-gas line, which coincides with the exact location of the roughening line. Its presence proves the existence of the preroughening transition in that model [2].

The partition function of the loop gas does not change when we modify the rules for placing the arrows on the loops. Consider the TBC $h(x+N,y)=-h(x,y)$. The seam is the vertical line across the entire cylinder where this boundary condition is being implemented. (Its location is gauge invariant; moving the seam and deforming it does not alter the partition function.) The columns on one side of the seam interpret the columns on the other side as being at height $-h$. In the arrow representation, this means that the direction of the arrow on each loop reverses each time that loop crosses the seam. There are two types of loops, homotopic and nonhomotopic. Nonhomotopic loops wrap around the cylinder in such a way that they cannot be contracted topologically into a point (like beads on a necklace). The requirement that the arrow on each loop reverses each time it crosses the seam is incompatible with nonhomotopic loops. The configurations with PBC's, $h(x+N,y)=h(x,y)$, are almost identical to those with TBC's, $h(x+N,y)=-h(x,y)$. Each homotopic PBC configuration is matched by a TBC configuration. Moreover, their Boltzmann weights are identical, since along the loop-gas line the reversal of arrows at the seam does not affect the Boltzmann factor. However, all nonhomotopic PBC configurations are absent for TBC's. Therefore, the free energies $f(+,0)$, and $f(-,0)$ are identical except for the contribution to $f(+,0)$ of configurations with nonhomotopic loops. Such configurations are suppressed in the $R_A(2m)$ and DOF $(2m)$ phases, because all loops are finite (all blue-lands are finite-sized lakes). This means that $\eta(-,0)=f(+,0)-f(-,0)$ vanishes in the thermodynamic limit exponentially fast with N. The latter is incompatible with reconstructional order, since $\eta(-,0)$ represents the free energy of a wall excitation in the $R_A(2m)$ phase, and therefore cannot be equal to zero. The loop gas cannot lie inside the $R_A(2m)$ phase.

To make this argument rigorous, we add the following aspect to the boundary conditions. Draw a second seam and associate a phase factor $\phi=\pi/2$ ($\phi=-\pi/2$) each time a loop

crosses this seam with an arrow pointing from left to right (right to left). These phase factors do not affect the Boltzmann factor of homotopic loops (the phases add up to zero), but they freeze out nonhomotopic loops [the phases add up to $\frac{1}{2}\pi$ mod(τ)]. Define free energies $\eta(\pm,a,\phi)=f(\pm,a,\phi)-f(+,0,\phi)$, with $a=0,\pm2,\pm4$, and $\phi=0,\pi/2$. From the above discussion it follows that, along with loop-gas line,

$$\eta(-,0,0)=\eta(+,0,\tfrac{1}{2}\pi) \tag{6}$$

for all even strip widths N. The twist boundary condition on the left creates a frustration of the Ising order, while the periodic-type boundary condition on the right is compatible with Ising order. This proves rigorously the absence of long-range Ising order along the loop-gas line. The loop-gas line cannot enter the $R_A(2m)$-reconstructed phase, nor either of the two RR phases. It cannot cross the Ising line in Fig. 1.

This is a rather weak result. In particular, it does not imply the absence of a RR phase because it does not exclude the possibility that the loop-gas line enters the rough phase. The implications of Eq. (6) become much stronger within the constraints of the weak-coupling hypothesis. Next, we summarize the scaling properties along every path the loop gas can follow through Fig. 3 and confront each with the loop-gas symmetry Eq. (6). This summary is important also for the numerical analysis in Sec. VI.

(i) Suppose the loop-gas line enters the deconstructed rough phase. The central charge is equal to $c=1$, and all the above surface free energies decay at large N as the inverse of the strip width with amplitudes that are linked to each other as

$$N\eta_s(+,a,\phi)\simeq\frac{K_G}{2}a^2+\frac{1}{2K_g}\phi^2,$$
$$N\eta_s(-,a,0)\simeq\frac{\pi}{4}. \tag{7}$$

The inverse of K_G, defined in Eq. (2), represents the surface roughness. The rough phase is described by the Gaussian fluctuations at large length scales, and these relations are exact and easy to derive in the Gaussian model. K_G must be smaller than $K_G<\pi/8$, since the KT roughening transition takes place at $K_G=\pi/8$. This is a factor 4 smaller than the conventional value $K_G=\pi/2$, because the step excitations create a height difference $dh=\pm2$ instead of $dh=\pm1$. The loop-gas identity Eq. (6), applied to Eq. (7), yields the value $K_G=\pi/2$, inconsistent with $K_G<\pi/8$. The loop-gas line cannot enter the deconstructed rough phase. [This argument proves also that point P in Fig. 1 must coincide with the KT transition into the $F(n+\frac{1}{2})$ phase.]

(ii) Suppose the loop-gas line moves along the Ising surface inside the rough phase, in particular the phase boundary with the RR phase dominated by (2,0)-type steps. At Ising critical points the central charge is equal to $c=0.5$ and the Ising Bloch wall free energy scales as a power law with universal amplitude

$$N\eta_i\simeq\pi/4. \tag{8}$$

The central charges and universal amplitudes add up, as $c=1.0+0.5=1.5$, when the Ising and roughening degrees of freedom interact weakly. The roughness degrees of freedom behave as in Eq. (7), with $K_G\leqslant\pi/8$, and the Ising degrees of freedom as in Eq. (8). This leads to the following FSS amplitudes:

$$N\eta(+,2,0)\simeq N\eta_s(+,2,0)\simeq 2K_G,$$
$$N\eta(-,0,0)\simeq N[\eta_s(-,0,0)+\eta_i]\simeq\tfrac{1}{2}\pi,$$
$$N\eta(-,2,0)\simeq N[\eta_s(-,0,0)+\eta_i]\simeq\tfrac{1}{2}\pi, \tag{9}$$
$$N\eta(+,0,0)_o\simeq N\eta_i\simeq\tfrac{1}{4}\pi,$$
$$N\eta(+,2,0)_o\simeq N[\eta_s(+,2,0)_o+\eta_i]\simeq 2K_G+\tfrac{1}{4}\pi.$$

The loop-gas identity Eq. (6), applied to Eq. (9), yields the value $K_G=\pi/4$, still too large compared to $K_G\leqslant\pi/8$. The loop-gas line cannot move along the Ising plane inside the rough phase. Along the opposite Ising plane, the phase boundary with the RR phase dominated by $(2,\pi)$ steps, the scaling relations are similar, with the two types of steps reversing roles.

(iii) Suppose the loop-gas line follows the line segment A-B in Fig. 3. The roughening and Ising degrees of freedom still couple weakly. The central charge remains equal to $c=1.5$, and the wall free energy scales still as $N\eta_i\simeq\frac{1}{4}\pi$, but the surface roughness is constant, $K_G=\pi/8$ [4]. The FSS amplitudes are similar to those in Eq. (9). The major difference is that the amplitudes for the two types of steps are identical by symmetry,

$$N\eta(+,2,0)\simeq N\eta(+,2,0)_o\simeq 2K_G. \tag{10}$$

The two interface free energies in Eq. (6) behave the same as in (ii). This again yields the value $K_G=\pi/4$, inconsistent with $K_G=\pi/8$. The loop-gas line cannot move along line segment A-B.

(iv) Suppose the entire loop-gas line lies inside the DOF phase. The FSS central charge estimates decay to $c\to0$. Both step free energies are nonzero. The Ising-wall-type free energy is equal to zero. However, the convergence becomes extremely slow when the Ising and roughening lines approach each other closely. The asymptotic forms will not be reached, and the apparent scaling will be almost indistinguishable from (ii) or (iii). For $\Delta\neq0$, the effective scaling behavior will be almost identical to that in Eq. (9), but still be distinguishable; the surface roughness cannot exceed the value $K_g=\pi/8$. For $\Delta=0$, the effective scaling behavior will be identical to that for (iii). This is a fundamental dilemma in studies of this type of phenomena. The only distinction between scenarios (iii) and (iv) is a judgment call on whether the two lines merge or not in the numerical analysis. In our case, Eq. (6) resolves the issue. It excludes (ii) but allows (iv).

In summary, the loop-gas symmetries exclude all the above scenarios except the last one. The only possibilities are the following: either the roughening and Ising lines approach each other pathologically closely, or the roughening and reconstruction degrees of freedom interact strongly and thus circumvent the above arguments. In any case, the Ising line can never cross the loop-gas line, since that aspect does not require the weak-coupling hypothesis.

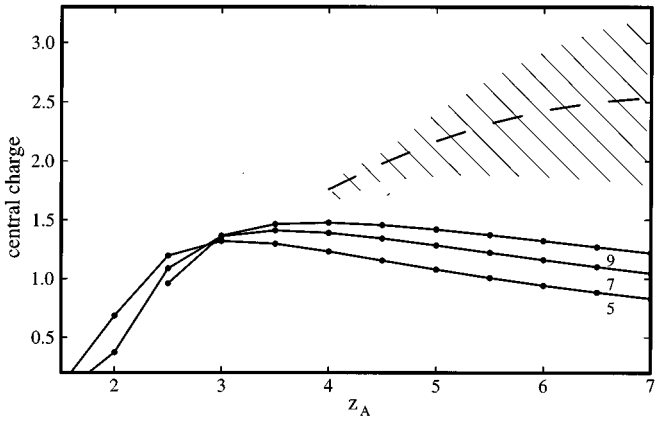

FIG. 5. FSS estimates for the central charge along the loop gas line for strip widths $N \leqslant 10$. The shaded area represents a conservative estimate for the uncertainty in the extrapolated values (the dashed line).

VI. NUMERICAL RESULTS

To distinguish between the scenarios outlined in Sec. V, we calculate the exact free energies $f(\pm,a,\phi)$ for semi-infinite lattices of width $2 \leqslant N \leqslant 10$, for several boundary conditions as defined in Sec. IV. We run the transfer matrix in the diagonal direction, where the state vector is 2^{2N} dimensional. Such strip widths are in the usual range for transfer matrix calculations. They might seem small for readers more familiar with Monte Carlo simulations, but realize that our values of $f(\pm,a,\phi)$ are accurate to better than 12 decimal places. There is no statistical noise, unlike MC simulations. This allows a very detailed FSS analysis that incorporates the leading corrections to scaling. It pays to trade system size for the ability to determine the leading corrections to scaling, because at criticality FSS corrections decay only as power laws. We know the exact location of the line where the reconstruction and roughening transitions must merge or cross (if they do), the FP loop-gas line $z_A = z_B + 1$. This makes our numerical analysis more accurate than earlier studies of the same type of phenomena.

Figure 5 shows the FSS estimates for the central charge $c(N)$ along the loop-gas line, $z_A = z_B + 1$. These values follow from the free energy with periodic boundary conditions $f(+,0,0)$ and the conformal field theory scaling relation

$$f(+,0,0)_N \simeq f_0 + \frac{\pi}{6N^2} c \tag{11}$$

as

$$c(N) = \frac{6}{\pi} \frac{(N^2-1)^2}{4N} [f(+,0,0)_{N-1} - f(+,0,0)_{N+1}]. \tag{12}$$

Equation (11) is valid at criticality. The $c(N)$ approximants of Eq. (12) must converge to zero away from criticality (exponentially fast). Indeed they do so inside the DOF $(2m)$ phase at small z_A. At criticality $c(N)$ must converge to the value characteristic for the universality class of the phase transition. In Fig. 5, we present the raw $c(N)$ data together with our best FSS estimates for c (the dashed line) and rather conservative error bars (the shaded area). At large z_A, the FSS corrections to scaling become large, and the FSS analysis of the type $c = c(N) + A/N^x$ becomes less reliable. The essential point is that c is certainly larger than $c = 1.5$. This contradicts all weak-coupling scenarios (see Sec. V). Maybe c varies continuously along the loop-gas line, but it is more likely that c is a constant between $2 \leqslant c \leqslant 3$, and that the variation of c in Fig. 5 reflects crossover scaling behavior between that value and $c = 1.5$ at the point where the roughening and Ising lines merge.

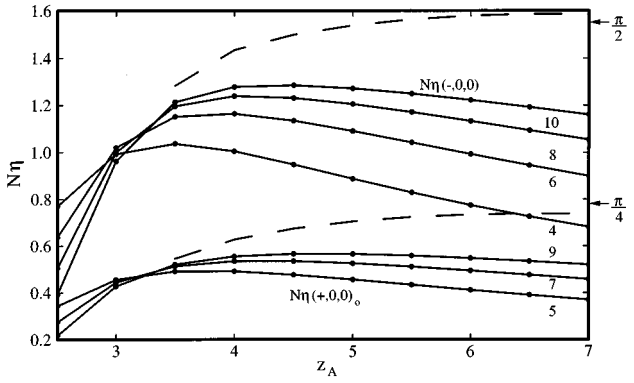

FIG. 6. $N\eta(+,0,0)_o$ [free energy of a $(0,\pi)$ wall] and $N\eta(-,0,0)$ [free energy of a $(0,\pi)$ wall with a twist in the surface] along the loop-gas line for strip widths $N \leqslant 10$.

Figure 6 shows the FSS scaling behavior of $N\eta(+,0,0)_o$ and $N\eta(-,0,0)$ along the loop-gas line. The first one forces an Ising wall into the reconstruction, and the second one an Ising wall and a twist in the surface. Both free energies vanish in the DOF $(2m)$ phase, as expected. At large z_A they scale with amplitudes that converge towards the values $N\eta(+,0,0)_o \simeq \pi/4$ and $N\eta(-,0,0) \simeq \pi/2$ (the dashed lines) consistent with the weak-coupling scenarios (ii)–(iv).

Figure 7 shows the FSS behavior of $N\eta(+,2,0)$ and $N\eta(+,2,0)_o$ along the loop-gas line. $N\eta(+,2,0)$ induces a (2,0)-type step in the surface and $N\eta(+,2,0)_o$ a $(2,\pi)$-type step. Both diverge in the DOF $(2m)$ phase as expected (the step free energies are finite). At large z_A, both decay as power laws. These data are inconsistent with scenarios (i) and (iii), in which $N\eta(+,2,0)$ and $N\eta(+,2,0)_o$ should become equal at large N. The results are inconsistent with scenario (ii) as well, since $N\eta(+,2,0)$ and $N\eta(+,2,0)_o$ should

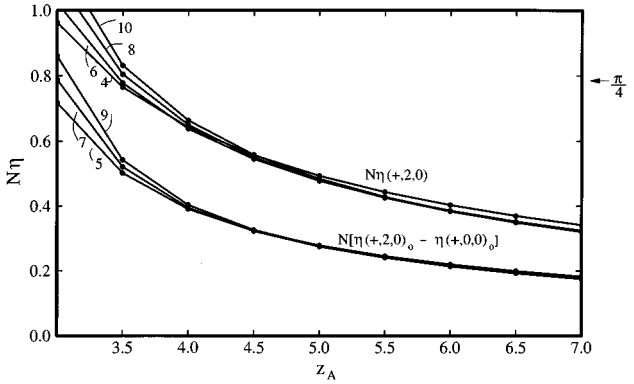

FIG. 7. $N\eta(+,2,0)$ [free energy of a (2,0) step] and $N\eta(+,2,0)_o - N\eta(+,2,0)_o$ [free energy of a $(2,\pi)$ step minus that of a $(0,\pi)$ wall] along the loop-gas line for strip widths $N \leqslant 10$.

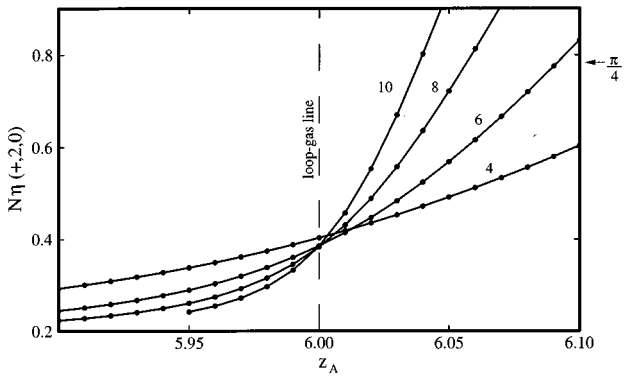

FIG. 8. The step free energy $N\eta(+,2,0)$ along the line $z_A+z_B=11$ for strip widths $N\leqslant 10$.

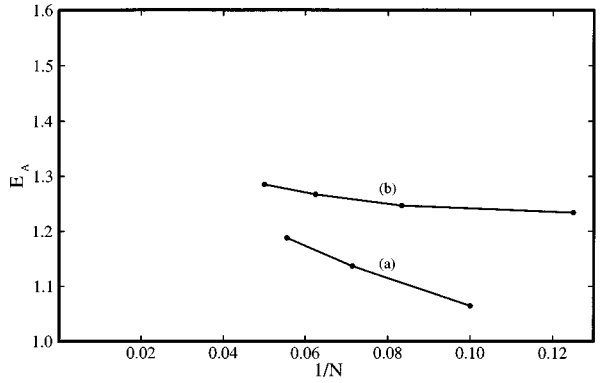

FIG. 9. FSS estimates for the location of the critical point $\exp(-E_c)=z_A=z_B+1$ along the loop-gas line from (a) the $N\eta(-,0,0)$ crossing points in Fig. 6, and (b) the $N\eta(+,2,0)=\pi/4$ points in Fig. 7.

differ by $\pi/4$ when the loop-gas line moves along the Ising plane inside the rough phase [see Eq. (9)]. To demonstrate this, in Fig. 7 we plot $N[\eta(+,2,0)_o-\eta(+,0,0)_o]$ instead of $N\eta(+,2,0)_o$ itself. The two sets of curves should fall on top of each other and converge towards a continuously varying roughness parameter $2K_G$. Instead, they differ by a factor close to 2. Most importantly, the data are inconsistent with scenario (iv), in which the roughening and Ising lines only approach each other asymptotically closely. We should find an effective scaling behavior of the form $N\eta(+,2,0)\simeq N[\eta(+,2,0)_o-\eta(+,0,0)_o]\simeq 2K_G$, with an effective roughness $K_G\geqslant\pi/8$. Instead, not only do the two amplitudes differ by a factor 2, both sink well below $2K_G=\pi/4$. The surface roughness becomes too large by a factor of about 2.

Figure 8 shows an example of the FSS behavior of $N\eta(+,2,0)$ along the cut $z_A+z_B=11$ through the loop-gas line. There exists no RR phase on either side of the loop-gas line. In the reconstructed phase, $N\eta(+,2,0)$ must diverge, and in the rough and RR phases converge to $2K_G$. At the KT roughening transition, $2K_G$ must be equal to $2K_G=\pi/4$. The conventional method to determine the roughening temperature is to extrapolate the points where $N\eta(+,2,0)=\pi/4$ as a function of N. In Fig. 8, these points lie at the reconstructed side of the loop-gas line. They converge toward the loop-gas line at such a rate that power-law fits actually overshoot the loop-gas line. This might lead to the conclusion that the roughening line neither crosses nor merges with the loop-gas line. On the other hand, along the loop-gas line itself, the amplitude converges very well to a value much smaller than $\pi/4$. This behavior is similar to what happens at a conventional KT-type roughening transition if one tries to estimate T_c by extrapolating the points where the FSS amplitude is larger than the true critical value, $N\eta(+,2,0)=\pi/4+a$ with $a>0$. The FSS behavior in Fig. 9 strongly supports the absence of a RR phase. $N\eta(+,2,0)$ diverges everywhere on the reconstruction side of the loop-gas line. Roughening seem to take place exactly at the loop-gas line, but surprisingly at a surface roughness well above the universal KT value.

Figure 9 shows two types of estimates for the critical point where the roughening and Ising lines merge: the $N\eta(-,0,0)$ crossing points from Fig. 6, and the $N\eta(+,2,0)=\pi/4$ points from Fig. 7. The existence of crossing points in $N\eta(-,0,0)$ and $N\eta(+,0,0)_o$ (see Fig. 6) is quite significant. In the more global context of Fig. 1, these crossing points converge to the Ising-type reconstruction lines. (This is the conventional method to locate such critical lines.) Their presence along the loop-gas line implies that all FSS estimates for the Ising transition cross the loop-gas line. The existence of points along the loop-gas line where $N\eta(+,2,0)=\pi/4$ (see Fig. 7) is equally significant. These points converge to the KT roughening lines in Fig. 1. (This is the conventional method to determine such roughening lines.) Their presence along the loop-gas line implies that all FSS estimates for the roughening transition cross the loop-gas line as well (see also the discussion about Fig. 8). The Ising and roughening lines cross the loop-gas line from opposite directions. All finite N estimates for the Ising and roughening lines cross each other.

Both curves in Fig. 9 must converge to $E_c\to\infty$ if the roughening and Ising lines only approach each other asymptotically closely. This is very unlikely, although both curves are convex [the corrections to scaling behave as $E_A(N)=E_c/A/N^x$, with an exponent $x<1$]. A conservative estimate puts the critical point somewhere between $1.4<E_c<1.6$.

These numerical results contradict all weak-coupling scenarios, in particular the one where the roughening and Ising lines only approach each other pathologically closely, the only one allowed by the loop-gas symmetries of Sec. V. The most damaging evidence is that $N\eta(+,2,0)$ becomes too small by a factor 2. It seems too far fetched that this amplitude can rebound all the way back to $\pi/4$ at very large N. Moreover, the central charge is significantly larger than the weak-coupling value $c=1.5$. Finally, the FSS estimates for the Ising and roughening lines cross each other for all finite N, and lead to an estimate $E_c\simeq 1.5\pm 0.1$ for the point along the loop-gas line where they merge.

VII. CONCLUSIONS

In this paper, we study the phase diagram of the staggered six-vertex model from the perspective of the competition between surface roughening and reconstruction, and also in the context of unresolved issues about the scaling properties of CFT with central charge $c>1$. In Sec. III we review the weak-coupling hypothesis as encountered in previous studies of this type of interplay. In particular we show that a reconstructed rough (RR) phase must be present in typical $c(2\times 2)$

CsCl(100)-type surfaces. The staggered six-vertex model includes a fully packed loop-gas line (Sec. IV). Its special symmetries explain the absence of the RR phase in this particular model. In Sec. V, we prove that the Ising-type reconstruction line cannot cross the loop-gas line. Moreover, we demonstrate that within the context of the weak-coupling hypothesis the roughening line cannot cross the loop-gas line either. This would explain the results by Mazzeo, Carlon, and van Beijeren, and put them in agreement with the generic phase diagram Fig. 3. However, our numerical results contradict all weak-coupling scenarios. The Ising and roughening lines merge along the loop-gas line. The central charge is large, at least equal to $c=2$ (see Fig. 5), and the surface roughness increases to a value about twice as large as the universal KT value (see Fig. 7).

Equations (4) and (5) represent FP loop gases on a square lattice. The FP loop-gas model on a honeycomb (HC) lattice, and a four-coloring problem on the square lattice, are related to this. Those models have large central charges as well, respectively $c=2$ and 3 [24–26]. Unfortunately they seem more closely related to Eq. (4) than Eq. (5). The partition function of the FP loop gas on a HC lattice is similar to Eq. (4), with three types of ''bridge energies'' instead of two, $z_\alpha=\alpha=A$, B, and C (the plaquettes of the HC lattice form three sublattices instead of two). Point P in our phase diagram is a critical point with central charge $c=1$. It is the meeting point of two DOF phases and also the point where the $E_A=E_B$ surface roughens (see Fig. 1). The corresponding point in the FP loop gas on the HC lattice, $z_A=z_B=z_C$, is a critical point with central charge $c=2$ [24–26]. It is the meeting point of three DOF phases, and of three critical lines with central charge $c=1$ (the phase boundaries between pairs of DOF phases) [27]. The scaling properties along $z_A=z_B\pm1$ in Fig. 1 appear to be more complex than this. This is not surprising, since Eq. (5) includes negative Boltzmann weights.

We close with some speculations about the origin of strong-coupling scaling along the loop-gas lines $z_A=z_B\pm1$. It might represent an interesting type of conformal field theory with $c>1$. More likely, it represents a conventional CFT, but one in which more degrees of freedom become critical than in Eq. (3) and Fig. 3. The obvious candidate is the Ising degree of freedom of the $R(2m+1,\theta)$ phase located on the opposite side of the $E_A=E_B$ line in Fig. 1. The two reconstructed phases do not seem to meet in Fig. 1, but they actually do so via the ''backdoor''. They meet at point $x=1$ in Eq. (5), since $z_A=z_B+1$ and $z_B=z_A+1$ are each other's analytic continuations. A four-state clock model coupled to a solid-on-solid model describes both types of reconstructions simultaneously. The $\sigma=\pm1$ Ising spins in Eq. (3) denote which of the two A-type sublattices is on top in the $R(2m,\theta)$ phase. Their generalizations are four-state clock variables, $\theta=0$, $\pm\frac{1}{2}\pi$, π, that point in the direction of the polarization of the arrows in vertex states 1–4 in Fig. 4(a). They denote which of the four sublattices is on top: one of the two A-type sublattices, $\theta=0,\pi$; or one of the two B-type sublattices, $\theta=\pm\frac{1}{2}\pi$. Such a model has ample room for conventional CFT's with central charge $c\geqslant2$. The loop-gas symmetries will enforce a nongeneric path through its phase diagram. Point $x=1$ in Eq. (5), where the two reconstructions meet, is almost certainly a critical point with central charge $c=2$. Figure 3 applies when $x=1$ is an isolated critical point. In that case, the Ising and roughening lines cannot meet until $x=1$ (our exact results of Sec. V). Instead, our numerical analysis shows that $x=1$ is not an isolated point. The next step will be an analytic calculation, to determine the scaling properties at point $x=1$. The critical dimension of the crossover operator in the loop-gas direction must be irrelevant or marginal for the loop-gas to remain critical until point S in Fig. 1. This line segment is probably some sort of Baxter-line coupled to roughening, since the universal amplitudes of both step free energies in Fig. 7 vary continuously.

ACKNOWLEDGMENTS

It is a pleasure to thank Enrico Carlon, Giorgio Mazzeo, and Henk van Beijeren for many discussions. This research was supported by NSF Grant No. DMR-9205125.

[1] G. Mazzeo, E. Carlon, and H. van Beijeren, Phys. Rev. Lett. **74**, 1391 (1995).
[2] M. den Nijs and K. Rommelse, Phys. Rev. B **40**, 4709 (1989); M. den Nijs, Phys. Rev. Lett. **64**, 435 (1990).
[3] For a review, see M. den Nijs, in *Phase Transitions and Adsorbate Restructuring at Metal Surfaces*, edited by D. King, The Chemical Physics of Solid Surfaces Vol. 7 (Elsevier, Amsterdam, 1994).
[4] M. den Nijs, Phys. Rev. B **46**, 10 386 (1992).
[5] Enrico Carlon, Ph.D. thesis, University of Utrecht, The Netherlands, 1996 (unpublished).
[6] Henk van Beijeren, Enrico Carlon, and Giorgio Mazzeo (private communication).
[7] T. C. Halsey, J. Phys. C **18**, 2437 (1985).
[8] J. M. Thijssen and H. J. F. Knops, Phys. Rev. B **37**, 7738 (1988); **42**, 2438 (1990).
[9] E. Granato and M. P. Nightingale, Phys. Rev. B **48**, 7438 (1993).
[10] Y. M. M. Knops, B. Nienhuis, H. J. F. Knops, and H. W. J. Blote, Phys. Rev. B **50**, 1061 (1994).
[11] M. P. Nightingale, E. Granato, and J. M. Kosterlitz, Phys. Rev. B **52**, 7402 (1995).
[12] P. Olsson, Phys. Rev. Lett. **75**, 2758 (1995).
[13] H.-J. Xu and B. W. Southern, J. Phys. A **29**, L133 (1996).
[14] A. B. Zamolodchikov, Pis'ma Zh. Eksp. Teor. Fiz. **43**, 565 (1986) [JETP Lett. **43**, 730 (1986)].
[15] I. Affleck, Phys. Rev. Lett. **56**, 746 (1986).
[16] H. van Beijeren, Phys. Rev. Lett. **38**, 993 (1977).
[17] H. van Beijeren and I. Nolden, in *Structures and Dynamics of Surfaces*, edited by W. Schommers and P. von Blanckenhagen (Springer, Berlin, 1987), Vol. 2.
[18] E. H. Lieb and F. Y. Wu, in *Phase Transitions and Critical Phenomena*, edited by C. Domb and M. S. Green (Academic, London, 1972).
[19] H. J. F. Knops, J. Phys. A **8**, 1508 (1975).

[20] M. Kohmoto, M. den Nijs, and L. P. Kadanoff, Phys. Rev. B **24**, 5229 (1981).
[21] A. B. Zamolodchikov and V. A. Fateev, Yad. Fiz. **32**, 581 (1980) [Sov. J. Nucl. Phys. **32**, 298 (1980)].
[22] T. T. Truong and M. den Nijs, J. Phys. A **19**, L645 (1986).
[23] R. J. Baxter, S. B. Kelland, and F. Y. Wu, J. Phys. A **9**, 397 (1976).
[24] H. W. J. Blote and B. Nienhuis, Phys. Rev. Lett. **72**, 1372 (1994); **73**, 2787 (1994).
[25] J. Kondev and C. L. Henley, Phys. Rev. Lett. **73**, 2786 (1994); Phys. Rev. B **52**, 6628 (1995).
[26] J. Kondev, J. de Gier, and B. Nienhuis, J. Phys. A **29**, 6489 (1996).
[27] D. Davidson and M. den Nijs (unpublished).